On the Relationship Between Carrier Mobility and Velocity in Sub-50 nm MOSFETs via Calibrated Monte Carlo Simulation

Osama M. Nayfeh*, Shaofeng Yu*, Dimitri A. Antoniadis*

* Microsystems Technology Laboratories, Massachusetts Institute of Technology, Cambridge, MA 02139
onayfeh@mtl.mit.edu, shaofeng.yu@ti.com, daa@mtl.mit.edu

Abstract

Subsequent to accurate 2D inverse modeling in the regime sensitive to electrostatics of industrial sub-50 nm NMOSFETs, a 2D full-band Monte Carlo device simulator was calibrated in the regime sensitive to transport parameters. The relationship between electron mobility and high-electric-field velocity at the maximum of the source-channel potential energy barrier was investigated. The results show a strong correlation, as was demonstrated previously experimentally. Moreover, further proof is provided that the velocity at which carriers are injected from the source region in modern NMOSFET's is only about half of the limiting thermal velocity.

1 INTRODUCTION

The expression for drive current in a MOSFET, I_{on}, can be written as

$$I_{on} = WQ_i(x_0)\langle v(x_0)\rangle . \quad (1)$$

Q_i (x_0) is the density of carriers at x_0 (CB peak) and $\langle v(x_0)\rangle$, is the average velocity of carriers in the channel direction [1]. Despite the dependence of I_{on} to velocity saturation and overshoot in the high-lateral field regime, previous experimental results of mechanical stress of the channel of a sub-50 nm MOSFETs, have shown there exists a significant correlation between low-field mobility, $\mu=q/(m^*\langle\tau\rangle$ and high-field velocity [2]. Also it was shown experimentally that the near-source velocity is ~40% of the limiting thermal velocity [3]. In this study we performed calibrated Monte Carlo simulation to confirm these experimental findings.

2 2D Inverse Modeling: Electrostatic Sensitivity

2D inverse modeling (IM)[4], using a continuum simulator was performed in the regime that is sensitive to electrostatics and relatively insensitive to transport to fully characterize a sub-50 nm NMOSFET, (SS=120mV/dec, DIBL=100 mV/V).

T_{ox}=1.5 nm (T_{ox_inv}=2.4 nm), and poly-gate concentration were determined by matching $C_{gg}=\partial Q_g/\partial V_g$ [4]. The density gradient model was used for QM effects. Short channel 2-D dopant profiles, of a deeply scaled NMOSFET were determined by the coupled IV & CV IM technique [9]. Leff was defined where the dopant concentration is $2x10^{19}$ cm^{-3}, and is ~40 nm. A series resistance R_{sd}=220 Ω·µm was then extracted and the measured I_{ds} vs V_{gs} data was corrected for R_{sd} [4].

3 Calibration of Monte Carlo Device Simulator: Transport Sensitivity

The full-band Monte Carlo simulator (MOCA) considers f and g type intervalley X-X phonon scattering, X-L intervalley phonon scattering, surface roughness, and ionized impurity scattering [5]. QM effects are included via self-consistent coupling of the Schrödinger equation [6].

The surface roughness scattering rate, τ_{sr} is derived from a statistical exponential autocovariance function [7]. Δ is the rms height of the amplitude roughness and L is the correlation length. The statistical parameters Δ and L of τ_{sr} [7] were adjusted to calibrate the surface roughness scattering rates, so that a good match achieved between the measured and Monte Carlo simulated low-lateral field I_{ds} vs. V_{gs} of the Leff ~40 nm NMOSFET under conditions of strong inversion.

Screened impurity scattering rates in MOCA are calculated using the Ridley statistical model [8]. No modifications were needed to the impurity scattering model in the low-field fit. Moreover, the Ridley impurity scattering model used was compared to a screened impurity analytical model independently developed from experimental data [9]. Fractional screened impurity scattering rates as a function of integrated channel charge N_i for a constant doping level of 2.5×10^{18} were compared between the two models. The fractional screened impurity scattering rate is defined as τ_{imp}/τ_{tot} where τ_{imp} is the impurity scattering rate and τ_{tot} is the total scattering rate. The results are in good agreement as shown in Fig. 1.

The acoustic phonon parameters used to compute phonon scattering rates are those referenced by Tang and Hess [10]. No changes were needed to the acoustic phonon parameters. Using the calibrated scattering rates from the low-lateral field fit, and the default phonon parameters from Tang and Hess [10], a good match is obtained between the measured I_{ds} vs V_{gs} characteristics corrected for R_{sd} under high lateral field conditions (V_{ds}=1.0 V) and Monte Carlo simulation. The fit is shown in Fig. 2.

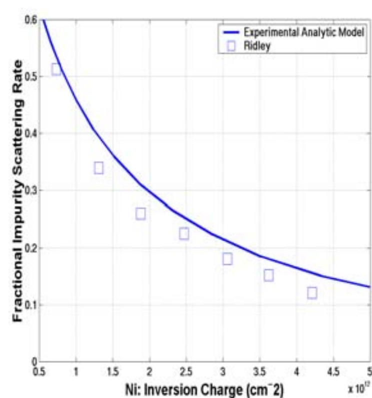

Fig. 1. Fractional impurity scattering rates vs. Ni, for an experimentally developed model [9] and the Ridley model [8].

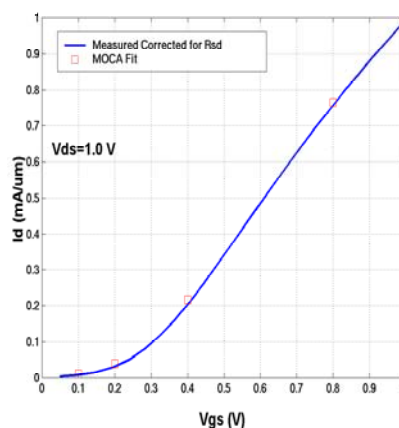

Fig. 2. High-lateral field Id. Vs. Vgs (measured and fit). The measured data is corrected for Rsd as described earlier.

4 How Close to the Thermal Limit

A reliable experimental method of extracting the electron velocity very close to the conduction band peak was demonstrated previously, and this velocity was determined to be no more than ~40% of the limiting thermal velocity ν_T for a deeply scaled Leff ~40 nm 1V NMOSFET [3].

To determine the mean free path, accurate scattering rates are needed. Each scattering rate, τ, was computed as a y-position (depth) dependent value, $\tau(y)$, weighted by the inversion charge density n(y) and is given by $\tau=\int(\tau(y)\cdot n(y)\cdot dy)/\int(n(y)\cdot dy)$ and shown in Fig. 3.. The position dependent vector mean free path in the direction of the channel $\boldsymbol{\lambda}$ is calculated with V_{DS}=1.0V, across the length of the device as $\boldsymbol{\lambda}=<(1/\tau)\cdot\mathbf{v}>$ [11], and is shown in Fig. 4. The value is about 0.3 nm at the conduction band peak region, which is much less than the length of the k_BT/q potential drop for this device, ~5 nm. We thus conclude that this device operates far from the ballistic limit.

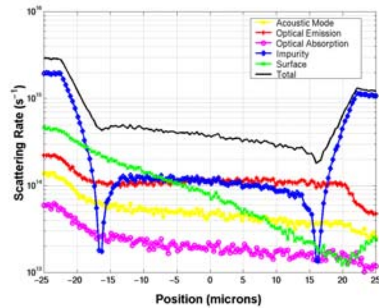

Fig. 3. Scattering rates along the length of the device ($V_{GS}=V_{DS}$=1.0V)

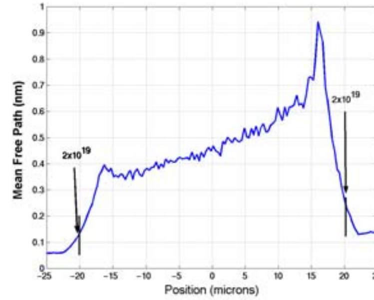

Fig. 4. Mean free path λ across the length of the device. Shown are the points where the doping=$2\text{x}10^{19}$ cm^{-3}. ($V_{GS}=V_{DS}$=1.0V)

The average velocity of carriers at the source-channel potential energy barrier, $<\nu(x_0)>$, was calculated as a weighted average of the position dependent velocity and inversion charge density $<\nu(x_0)>=\int(\nu(y)\cdot n(y)\cdot dy)/\int(n(y)\cdot dy)$ with V_{DS}=1V.

Since the thermal velocity ν_T is dependent on inversion charge density [2], V_{gs} was varied, and the value of $<\nu(x_0)>$, was compared with the thermal velocity, as shown in Fig. 5. Monte-Carlo simulation under ballistic tranport conditions was performed to determine ν_T. The results in Fig. 5 demonstrate that the device operates at only 45-55% of the thermal velocity limit as was shown previously experimentally.

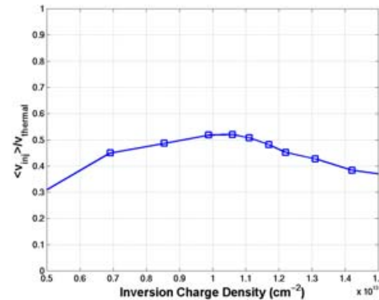

Fig. 5. The ratio $<\nu(x_0)>/\nu_T$ as a function of inversion charge density.

5 Relationship Between Low-Field Carrier Mobility and High-Field Velocity

Significant correlation between low-field mobility and high-electric field velocity has been demonstrated experimentally by uniaxial strain applied via mechanical bending of deeply scaled NMOSFETs. It was shown that the measured dependence of near-source electron velocity $\langle v(x_0) \rangle$ on low-field mobility μ_{eff}, $R_{v,\mu}=\delta\langle v(x_0)\rangle/\delta\mu_{eff}$ is about 0.45 [2]

The surface-roughness scattering rate parameters Δ and L [7], were modified from their calibrated values to give a 13% change in the effective short-channel mobility (μ_{eff}). No changes were made to the saturation velocity or to the impurity scattering model [8]. A more proper study would include band-structure changes due to strain. The impact of the surface mobility enhancement on the scattering rates is shown in Fig 6.

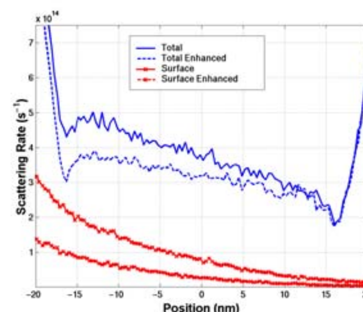

Fig. 6. Surface scattering and total scattering rate across the length of the inverse modeled device in Fig. 1 with enhanced surface mobility.

The effective short-channel mobility change can be defined as the percent change in current in the linear regime $\delta\mu_{eff} = \Delta Id_{lin}/Id_{lin}$ with V_{gs}=1Vand V_{ds}=50mV [13]. A V_{ds}=1.0 V was then applied to simulate the device in the high-electric field regime, and $\delta\langle v(x_0)\rangle = \Delta Id_{sat}/Id_{sat}$= was evaluated. Therefore, Monte-Carlo simulation gives a value of $R_{v,\mu}=\delta\langle v(x_0)\rangle/\delta\mu_{eff}=0.43$, which agrees well with the value of $R_{v,\mu}=0.45$ from the previous experimental results. Thus, despite the high-field transport phenomenon, the drain current in a modern MOSFET is indeed significantly correlated to low-field mobility.

References

[1] M. Lundstrom and Z. Ren, IEEE TED, vol. 49, pp. 133-141, Jan 2002.
[2] A. Lochtefeld and D. Antoniadis, IEEE EDL, vol. 22, pp. 591-593, Dec. 2001.
[3] A. Lochtefeld and D. Antoniadis, IEEE EDL, vol. 22, pp. 95-97, Feb. 2001.
[4] I. Djomehri and D.A. Antoniadis, IEEE TED, vol. 49, pp. 568-575, April. 1998.
[5] A. Duncan, U. Ravaioli, and J. Jakurmeit, IEEE TED, vol. 45, pp. 867-876, April. 1998.
[6] B. Winstead, H. Tsuchiya, U. Ravaioli, Nanotech 2001, pp. 566-569.
[7] Yamakawa, et al., Miyatsuji, Masaki, and Ravaioli, JAP, vol. 79, pp. 911-916, Jan. 1996.
[8] B.K. Ridley, J. Phys. C, vol. 10, pp. 1589–1593, 1977.
[9] H.M..Nayfeh, C.W. Leitz, A.J. Pitera, E.A. Fitzgerald, J.L. Hoyt, D.A. Antoniadis, IEEE EDL., vol 24, pp. 248-250, April 2003.
[10] J.Y. Tang and Karl Hess, JAP, vol. 54, pp. 5139-5144, Sep. 1983.
[11] Jungemann, Meinerzhagen "Hierarchial Device Simulation," Springer Engineering 2003.
[12] K. Natori, JAP, vol.. 76, pp. 4879-4890, 1994.
[13] Lundstrom, Mark, IEEE EDL., vol. 22, pp. 293-295, June 2001.